Plasma Vertical Stabilization in the Presence of Coil Voltage Saturation in the DIII-D Tokamak*

E. Schuster†, M. L. Walker‡, D. A. Humphreys‡ and M. Krstić†

† Department of Mechanical and Aerospace Engineering, University of California at San Diego
9500 Gilman Dr., La Jolla, CA 92093-0411
schuster@mae.ucsd.edu krstic@ucsd.edu

‡General Atomics
P.O. Box 85608, San Diego, CA 92186-5608
walker@fusion.gat.com dave.humphreys@gat.com

Abstract

An anti-windup compensator is implemented for a given nominal plasma vertical controller guaranteeing global vertical stabilization of the plasma in the presence of actuactor saturation for all reference commands. The anti-windup synthesis problem is to find a nonlinear modification of the nominal linear controller that prevents vertical instability and undesirable oscillations but leaves the nominal closed loop unmodified when there is no input saturation.

1 Introduction

The Advanced Tokamak (AT) operating mode is the principal focus of the DIII-D tokamak. Demands for more varied shapes of the plasma and requirements for high performance regulation of the plasma boundary and internal profiles are the common denominator of the AT operating mode in DIII-D [1]. In order to be prepared for the higher control demands arising in AT scenarios, current efforts are focused on the development of an integrated multivariable controller [2] to take into account the highly coupled influences of equilibrium shape, profile, and stability control. The first step of this project is the design of the shape and vertical controller which will be integrated in the future with control of plasma profiles. The time-scale properties of the system allow the separation of the vertical stabilization problem, which is the focus of this paper, from the shape control problem.

The problem of vertical and shape control in tokamaks was and is still extensively studied in the fusion community. A recent summary of the existing work in the field can be found in [3]. Several solutions for the design of the nominal controller were proposed for different tokamaks using varied control techniques based on linearized models. However, only a few of them [4] take into account the control voltage constraint in the design of the nominal controller. The goal of this paper is not the design of the nominal controller but the design of an anti-windup compensator that blends any given nominal controller, which is designed to fulfil some local performance criterion, with a nonlinear feedback designed to guarantee stability in the presence of input saturation but not necessarily tuned for local performance.

The shape control methodology at DIII-D is based on "isoflux control". The isoflux control method, now in routine use on DIII-D, exploits the capability of the real time EFIT plasma shape reconstruction algorithm to calculate magnetic flux at specified locations within the tokamak vacuum vessel. Figure 1 illustrates a lower single null plasma which was controlled using isoflux control. Real time EFIT can calculate very accurately the value of flux in the vicinity of the plasma boundary. Thus, the controlled parameters are the values of flux at prespecified control points along with the X-point r and z position. By requiring that the flux at each control point be equal to the same constant value, the control forces the same flux contour to pass through all of these control points. By choosing this constant value equal to the flux at the X-point, this flux contour must be the last closed flux surface or separatrix. The desired separatrix location is specified by selecting one of a large number of control points along each of several control segments. An X-point control grid is used to assist in calculating the X-point location by providing detailed flux and field information at a number of closely spaced points in the vicinity of the X-point.

*This work was supported in part by grants from UCEI and NSF and by DoE contract number DE-AC03-99ER54463.

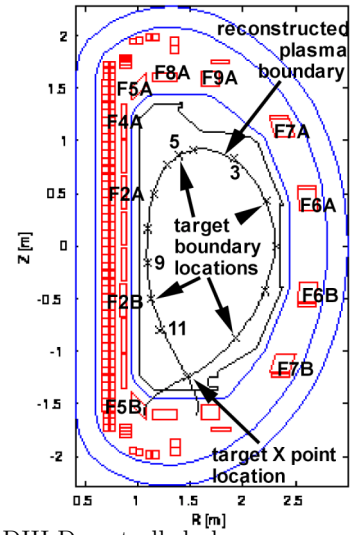

Figure 1: DIII-D controlled plasma parameters in isoflux control (r_x, z_x and flux at control points).

Time-scale separation of vertical and shape control appears to be critical for DIII-D, since multivariable shape controllers can require significant computation. Figure 2 shows the closed loop system comprised of the DIII-D inner plant and a stabilizing controller. This system is stable locally (when there is no input saturation) and the 6 coil currents F2A, F2B, F6A, F6B, F7A, and F7B are approximately controlled to a set of input reference values. As a result, this system can act as an inner control loop for the shape control. Figure 2 shows that the inner loop provides as input actuators the 6 vertical coil current reference signals, the centroid vertical position reference signal and up to 12 shape coil command voltages. A method implemented for sharing actuators involves constructing a linear controller which simultaneously stabilizes and provides control of vertical control coil currents on a fast time scale. By integrating control of the vertical control coils into a stabilizing controller, conflicts between shape and vertical control use of these coils is eliminated. "Frequency sharing" is accomplished explicitly with an H-infinity loop shaping design by weighting low frequencies to regulate the coil currents and high frequencies to stabilize the plasma. The design technique ensures robust stability. To take into account the nonlinear nature of the power supplies we remove the linearized model of the choppers from the inner plant and incorporate a full nonlinear model of them into an augmented saturation block as it is shown in Figure 2. The nominal linear vertical controller is synthesized now using no information of the choppers and its output now represents directly the desired coil voltages. A chopper inverse function computes the necessary command voltages within the saturation levels to make the output voltage of the choppers equal to the desired coil voltages. When the chopper inverse funtion fails calculating those command voltages we say we have saturation.

Although the saturation levels of the command voltages are still fixed values (±10 V), the saturation levels of the augmented saturation block are now functions of time (coil load current and DC supply voltage V_{ps}).

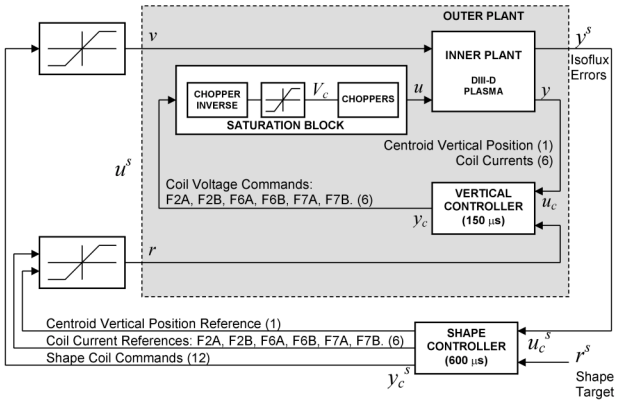

Figure 2: Plant architecture.

In order to make this approach successful the inner controller (vertical controller) must guarantee the stability of the plant for all commands coming from the outer controller (shape controller). Due to the constrained control, the nominal linear vertical controller may fail to stabilize the vertical position of the plasma inside the tokamak when large or fast disturbances are present or when the references coming from the shape controller change suddenly. Although the saturation of coil currents and voltages is a common problem in tokamaks and there are efforts to minimize the control demand for shape and vertical control and to avoid saturation [5, 6], the saturation of the actuators are generally not taken into account in the design of the nominal controllers in present works. The inner loop design must take care then of the windup of the actuators of that loop and ensure vertical stability for any command coming from the outer controller. The anti-windup synthesis problem is to find a nonlinear modification of the predesigned nominal linear controller that prevents vertical instability and undesirable oscillations but leaves the nominal closed loop unmodified when there is no input saturation. Due to the characteristics of our problem we follow the ideas introduced in the companion papers [7, 8] and also discussed in [9] for exponentially unstable systems. This technique has been shown to be successful in several case studies. However, the method must be modified and complemented in order to fulfill the performance requirements of our system.

The paper is organized as follow. Section 2 introduces the basis of the anti-windup method. The characteristics of our plant are presented in section 3. The control system design and some simulation results are combined in Section 4. Section 5 discusses some implementation issues and conclusions are presented in Section 6.

2 Anti-Windup Compensator Fundamentals

We consider exponentially unstable linear plants with control input $u \in \Re^m$ and measurements $y \in \Re^p$. We write the plant of our system in state-space form separating the stable modes ($x_s \in \Re^{n_s}$) from the exponentially unstable modes ($x_u \in \Re^{n_u}$) where the dimension of the state vector x is $n = n_s + n_u$,

$$\begin{aligned} \dot{x} &= Ax + Bu \quad (1) \\ \begin{bmatrix} \dot{x}_s \\ \dot{x}_u \end{bmatrix} &= \begin{bmatrix} A_s & A_{su} \\ 0 & A_u \end{bmatrix} \begin{bmatrix} x_s \\ x_u \end{bmatrix} + \begin{bmatrix} B_s \\ B_u \end{bmatrix} u \\ y &= Cx + Du. \quad (2) \end{aligned}$$

The eigenvalues of A_s have non-positive real part and the eigenvalues of A_u have positive real part. In addition, we consider that a nominal linear controller with state $x_c \in \Re^{n_c}$, input $u_c \in \Re^p$, output $y_c \in \Re^m$ and reference $r \in \Re^p$,

$$\begin{aligned} \dot{x}_c &= A_c x_c + B_c u_c + Gr \quad (3) \\ y_c &= C_c x_c + D_c u_c + Hr \quad (4) \end{aligned}$$

has been already designed so that the closed loop system with interconnection conditions

$$u = y_c, \quad u_c = y \quad (5)$$

is well posed and internally stable. When the controller output is subject to saturation, i.e. the interconnection conditions (5) are changed to

$$u = sat(y_c), \quad u_c = y, \quad (6)$$

the synthesis of an anti-windup scheme is necessary. In this case the interconnection conditions are modified to

$$u = sat(y_c + v_1), \quad u_c = y + v_2, \quad (7)$$

where the signals v_1 and v_2 are the outputs of the anti-windup compensator [9]

$$\begin{aligned} \dot{x}_{aw} &= Ax_{aw} + B[sat(y_c + v_1) - y_c] \quad (8) \\ v_1 &= (\beta(x_u) - 1)y_c \\ &\quad + \alpha[x_u - \beta(x_u)(x_u - x_{aw_u}), \beta(x_u)\kappa(x_{aw})] \quad (9) \\ v_2 &= -Cx_{aw} - D[sat(y_c + v_1) - y_c]. \quad (10) \end{aligned}$$

The anti-windup scheme is illustrated in Figure 3. In addition to modifying the nominal controller when input saturation is encountered, the anti-windup compensator modifies the closed loop if the exponentially unstable modes get close to the boundary of some reasonably large subset of the region where these unstable modes are controllable with the given bound on the control. The signal β is defined as

$$\beta(x_u) = \begin{cases} 1, & x_u \in \chi_{lower} \\ 0, & x_u \notin \chi_{upper} \end{cases} \quad (11)$$

and interpolated in between, where $\chi_{lower} \subset \chi_{upper}$ are subsets of χ, the domain of attraction of the disturbance-free system subject to the saturation of the output controller or what we call controllable region. The freedom to define χ_{lower} and χ_{upper} is a tool the designer has to deal with the disturbances that although not modeled are present in the system. The smaller χ_{lower} and χ_{upper}, the bigger the disturbances tolerated by the system without escaping the controllable region χ. One choice of the function $\alpha : \Re^{n_u} \times \Re^m \to \Re^m$ is given by

$$\alpha(\zeta, \omega) = K_u \zeta + \omega \quad (12)$$

where K_u is such that $A_u + B_u K_u$ is Hurwitz. The function $\kappa(x_{aw})$ is designed to improve the performance of the antiwindup scheme when the controller output is not saturating. It is important to note at this point that this scheme requires the measurement or estimation of the exponentially unstable modes x_u.

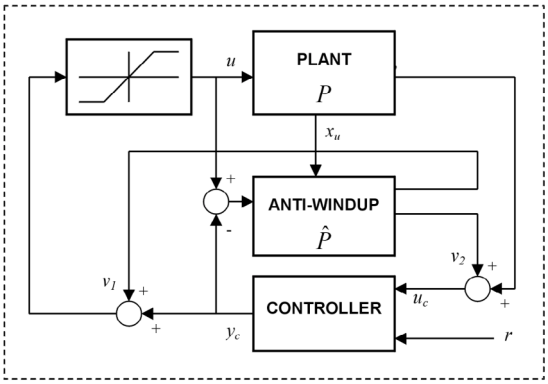

Figure 3: Anti-windup scheme.

3 Plant Characteristics

Before starting with the design of our control system it is necessary to state the main characteristic of our plant. Figure 2 illustrates the architecture of our plant. The dynamics of our plant can be written as

$$\begin{aligned} \dot{x} &= Ax + Bu + Ev + F \quad (13) \\ \begin{bmatrix} \dot{x}_s \\ \dot{x}_u \end{bmatrix} &= \begin{bmatrix} A_s & A_{su} \\ 0 & A_u \end{bmatrix} \begin{bmatrix} x_s \\ x_u \end{bmatrix} + \begin{bmatrix} B_s \\ B_u \end{bmatrix} u \\ &\quad + \begin{bmatrix} E_s \\ E_u \end{bmatrix} v + \begin{bmatrix} F_s \\ F_u \end{bmatrix} \\ y &= Cx + Du + Gv, \quad (14) \end{aligned}$$

where the vector u of dimension $m = 6$ are the voltage commands for power supplies on the vertical coils $F2A$, $F2B$, $F6A$, $F6B$, $F7A$ and $F7B$, the vector v of dimension $q = 12$ are the voltage demands for the shape coils, the vector y of dimension $p = 7$ consists of the six vertical coil currents and the plasma centroid position. Due to the composition of the output vector it is convenient to write the reference for the nominal controller as $r = [r_I \quad r_Z]^T$ where r_I are the current

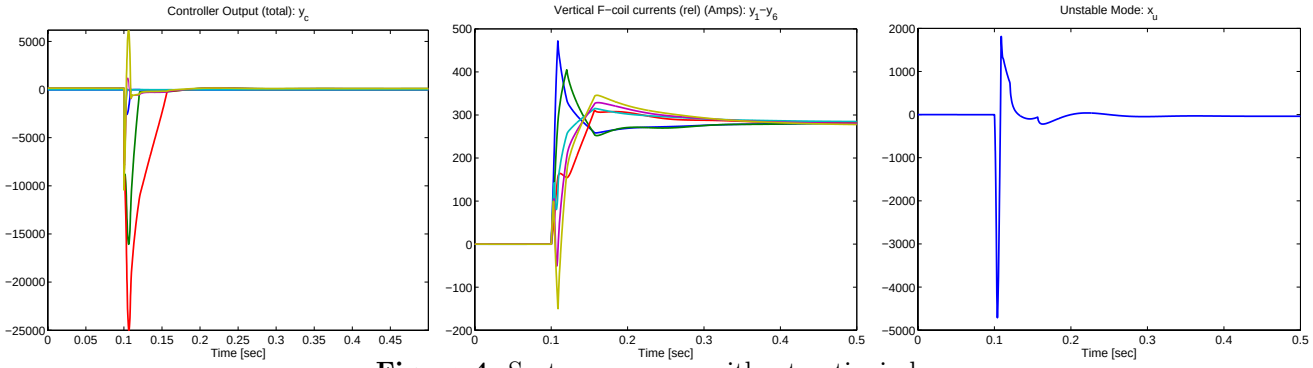

Figure 4: System response without anti-windup

references for the six vertical coils and r_Z is the centroid position reference. The main characteristics of our plant can be summarized as:

- There is only one unstable eigenvalue, i.e. $n_u = 1$, and the $n_s = n - 1$ stable eigenvalues are strictly negative. However, some of them are very close to zero (slow modes).
- The saturation of the channel i of the controller, for $i = 1 \dots m$, can be modeled as

$$sat(y_{c_i}) = \begin{cases} M_i^{max}(t) & \text{if } y_{c_i} \geq M_i^{max}(t) \\ y_{c_i}(t) & \text{if } M_i^{min}(t) < y_{c_i} < M_i^{max}(t) \\ M_i^{min}(t) & \text{if } y_{c_i} \leq M_i^{min}(t) \end{cases}$$

- There is no direct measurement of the unstable mode.
- The control input u is not the only input of the inner plant. In addition to the voltage commands u for the vertical coil from the vertical controller, there are voltage demands v for the shape coils coming from the shape controller.

Figure 4 shows the response of the closed loop without anti-windup compensator when r_{I_i} for $i = 1 \dots m$ are step functions of magnitude equal to 280 Amps. It is possible to note the large excursions of the controller output y_c. For step functions of higher magnitude the response diverges, i.e. stability is lost. Large excursions at the output of the controller must be eliminated and global stability must be guaranteed.

4 Control System Design

Controllable region definition: Given the dynamics of the unstable mode by the scalar equation

$$\dot{x}_u = A_u x_u + B_u u + E_u v + F_u, \tag{15}$$

we can compute the minimum and maximum values of the unstable mode that can be reached without losing control authority to stabilize the system,

$$x_u^{max} = \frac{-(B_u u)^{min} - E_u v - F_u}{A_u} \tag{16}$$

$$x_u^{min} = \frac{-(B_u u)^{max} - E_u v - F_u}{A_u}, \tag{17}$$

and define the controllable region as

$$\chi = \left\{ x_u : x_u^{min} \leq x_u \leq x_u^{max} \right\}. \tag{18}$$

The maximal and minimal control is given by

$$(B_u u)^{min} = \sum_{i=1}^{m} |B_{u_i}|\, g_i(-\text{sgn}(B_{u_i})) \tag{19}$$

$$(B_u u)^{max} = \sum_{i=1}^{m} |B_{u_i}|\, g_i(\text{sgn}(B_{u_i})) \tag{20}$$

where B_{u_i} is the i-th component of B_u and the function g_i is defined as

$$g_i(a) = \begin{cases} M_i^{max} & \text{if } a > 0 \\ M_i^{min} & \text{if } a < 0. \end{cases} \tag{21}$$

Once χ is determined, we can define

$$\chi_{lower} = \left\{ x_u : x_u^{min,l} < x_u < x_u^{max,l} \right\} \tag{22}$$

$$\chi_{upper} = \left\{ x_u : x_u^{min,u} < x_u < x_u^{max,u} \right\} \tag{23}$$

where $x_u^{min,l} = f^l x_u^{min}$, $x_u^{max,l} = f^l x_u^{max}$, $x_u^{min,u} = f^u x_u^{min}$, $x_u^{max,u} = f^u x_u^{max}$, and $0 < f^l < f^u < 1$. Once χ, χ_{lower} and χ_{upper} are defined, the function β adopts the shape shown in Figure 5.

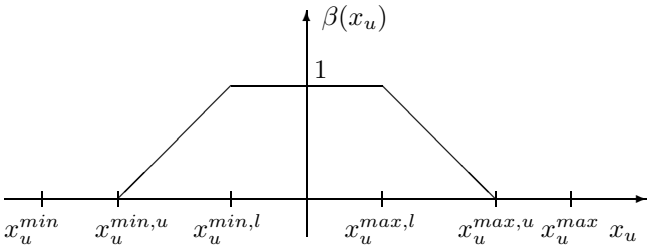

Figure 5: Beta function.

Design of gain K_u: The feedback gain K_u is designed such that

$$A_u + B_u K_u < 0 \tag{24}$$

$$\text{sign}(B_{u_i}) = -\text{sign}(K_{u_i}) \tag{25}$$

$$|K_{u_i} x_u^{max,u}| > \max(|M_i^{min}|, |M_i^{max}|) \tag{26}$$

$$|K_{u_i} x_u^{min,u}| > \max(|M_i^{min}|, |M_i^{max}|) \tag{27}$$

for $i = 1 \ldots m$ where B_{u_i} and K_{u_i} are the i-th components of B_u and K_u respectively. We guarantee in this way that for $x_u^{max,u} \leq x_u < x_u^{max}$ $(\beta(x_u) = 0)$ we have

$$B_u u = B_u \text{sat}(K_u x_u) = (B_u u)^{min} \tag{28}$$

and consequently that

$$\begin{aligned} \text{sign}(\dot{x}_u) &= \text{sign}(A_u x_u + B_u \text{sat}(K_u x_u) + E_u v + F_u) \\ &= sign(A_u x_u + (B_u u)^{min} + E_u v + F_u) \\ &< 0 \end{aligned} \tag{29}$$

by definition (16). In similar way we can show that for $x_u^{min} \leq x_u < x_u^{min,u}$ $(\beta(x_u) = 0)$ we have

$$\text{sign}(\dot{x}_u) > 0 \tag{30}$$

Conditions (29) and (30) ensures the stabilization of the unstable mode when $\beta(x_u) = 0$ through the signal $v_1 = -y_c + K_u x_u$.

Design of the function κ: Another important task in the design of the anti-windup is the definition of the function $\kappa(x_{aw})$. As we stated in previous sections, we design this function with the aim of making the states of the anti-windup compensator converge to zero as fast as possible when the unstable mode is in the "safe" region defined by the condition $\beta(x_u) = 1$ and no channel of the controller output is saturating. However, at this point we follow a non-standard procedure. Instead of designing the function κ, we make $\kappa(x_{aw}) = 0$ and modify the structure of the anti-windup compensator as follow

$$\begin{aligned} \dot{x}_{aw} &= A x_{aw} + B[sat(y_c + v_1) - y_c] \\ &- [1 - \gamma(abs(y_c + v_1))]\delta x_{aw}, \quad \delta > 0 \end{aligned} \tag{31}$$

where the function γ is an indication of saturation, being zero if none of the input channel is saturating and one otherwise. In this way, when the unstable mode is in the "safe" region and there is no saturation the dynamics of the anti-windup can be written as

$$\begin{aligned} \dot{x}_{aw} &= A x_{aw} + B v_1 - \delta x_{aw} \\ &= \begin{bmatrix} A_s - \delta I_s & A_{su} + B_s K_u \\ 0 & A_u + B_u K_u - \delta I_u \end{bmatrix} \begin{bmatrix} x_{aw_s} \\ x_{aw_u} \end{bmatrix} \\ v_1 &= K_u x_{aw_u} \\ v_2 &= -C x_{aw} - D v_1. \end{aligned}$$

where I_s and I_u are identity matrices of appropriate dimension. The rate of convergence of x_{aw} to zero can be regulated now by the gain δ. A scheme of the anti-windup design is shown in Figure 7.

Figure 6 shows now the response of the closed loop when r_{I_i} for $i = 1 \ldots m$ are step functions of magnitude equal to 840 Amps but this time with the anti-windup compensator working. Comparing figures 4 and 6 it is possible to note that even for a much larger reference step the excursion of the unstable mode x_u is much smaller, the huge excursion of the output of the controller y_c is eliminated, and the output response y does not exhibit any decrease of performance.

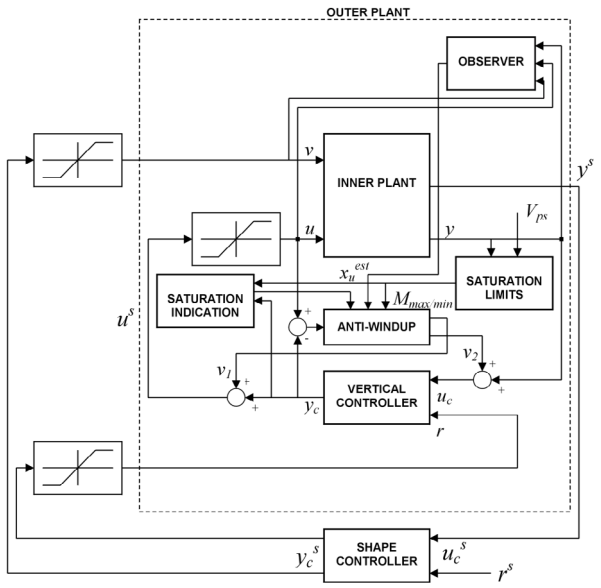

Figure 7: Inner loop anti-windup scheme.

5 Implementation issues

Observer A state observer is designed for the estimation of the unstable mode of the plant because a direct measurement is not available. A high gain observer is required in this case to ensure that the estimation is fast enough to prevent any excursion of the unstable mode outside the controllable region. Simulation studies show the effectiveness of the approach. This can be explained by the fact that an accurate estimation is not required to make the anti-windup compensator achieve its goals. It is important to realize that from the observer we only need to know if the unstable mode is inside χ_{lower} or outside χ_{upper}. In addition it is always possible to compensate the inaccuracy of the observer with a convenient selection of the design parameters f^l and f^u.

Robustness: The growth rate of the plant is directly related to the elongation of the plasma. The more elongated the plasma, the more unstable. This means that when we modify the shape of the plasma using the outer loop (shape controller), the plant of the inner loop is modified. However, the input-output relationship of the plant does not vary significatively when the growth rate varies. It is for this reason that the anti-windup compensator is very robust against changes in the growth rate. This same robustness is not exhibited by the observer because its operation is based on the state-space model and consequently on the growth

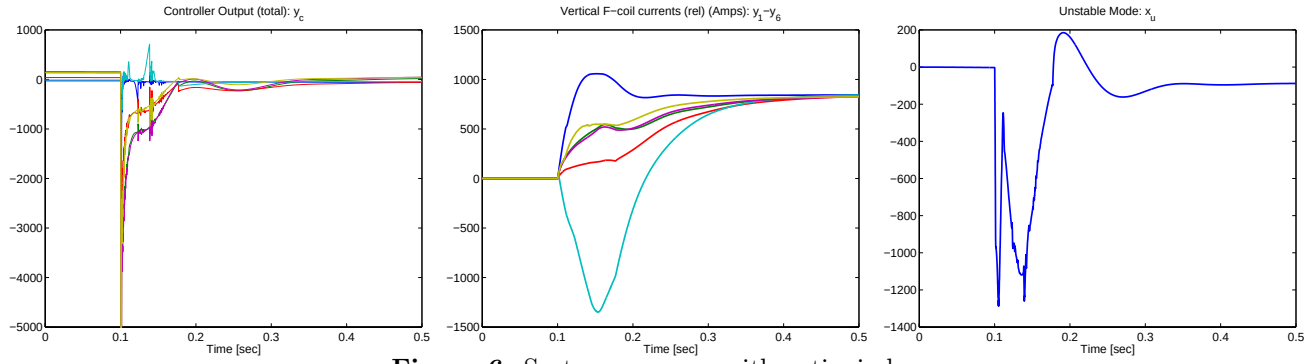

Figure 6: System response with anti-windup.

rate A_u. According to the value of the growth rate A_u, which can be computed on-line, different models are used for the estimation of the unstable mode.

Computational Effort: Due to the short time-scale of the inner loop the computational effort must be minimized. Although an observer scheduling is a must, simulation studies show that a very low order observer ($n_{obs} = 10$ states) succeeds in giving an estimation of the unstable mode which is good enough to prevent the vertical instability of the plant ($n = 123$ states). In addition a very low order anti-windup compensator ($n_{aw} = 20$ states) succeeds in providing the necessary input-output relationship even in the presence of uncertainties in the growth rate of the plant.

6 Conclusions

The proposed scheme has been shown in nonlinear simulations to be very effective in guaranteeing global stability of the inner loop in the presence of voltage saturation of the vertical coils. The scheme will be tested in experimental conditions. However, it is possible to anticipate at this stage the needing and convenience of a conditioning of the signals coming from the shape controller. A watch-dog will monitor the additional input v and keep it from making the controllable region in (16)–(17) shrink below a predesigned minimum size and from leaving suddenly the unstable mode outside the controllable region. In addition, a rate limiter on r_I will be implemented to take into account the characteristic integration time of the coils.

After succeeding in the vertical stabilization of the plasma in experimental conditions, efforts will be concentrated on the design of the outer loop. The necessity of a similar anti-windup scheme for the outer loop is anticipated; not only due to the inherent limitations of its actuators but also due to the fact that the inner loop will modify, through the watch-dog and rate limiter, the control signals of the outer loop in order to preserve stability of the inner plant and improve performance. In this case we will deal with a stable (stabilized by the inner loop design) but nonlinear plant.

Acknowledgments

The authors want to thank Andrew Teel and Luca Zaccarian for their valuable explanations and suggestions.

References

[1] J. L. Luxon, "A design retrospective of the DIII-D tokamak", *Nuclear Fusion*, **42**, pp. 614-33, 2002.

[2] D. A. Humphreys, M. L. Walker, J. A. Leuer and J. R. Ferron, "Initial implementation of a multivariable plasma shape and position controller on the DIII-D tokamak", *Proceedings of the 2000 IEEE International Conference on Control Applications*, Anchorage, Alaska, USA, pp. 385-94, September 2000.

[3] R. Albanese and G. Ambrosino, "Current, position and shape control of tokamak plasmas: A literature review", *Proceedings of the 2000 IEEE International Conference on Control Applications*, Anchorage, Alaska, USA, pp. 412-18, September 2000.

[4] L. Scibile and B. Kouvaritakis, "A discrete adaptive near-time optimum control for the plasma vertical position in a tokamak", *IEEE Transactions on control systems technology*, Vol.9, no.1, p. 148, 2001.

[5] G. Ambrosino, M. Ariola, A. Pironti, A. Portone and M. Walker, "A control scheme to deal with coil current saturation in a tokamak", *IEEE Transactions on control systems technology*, Vol.9, no.6, p. 831, 2001.

[6] R. Albanese, G. Ambrosino, A. Pironti, R. Fressa and A. Portone, "Optimization of the power supply demand for plasma shape control in a tokamak", *IEEE Transactions on magnetics*, Vol.34, no.5, p. 3580, 1998.

[7] A. R. Teel and N. Kapoor, "The $\mathcal{L}_2$ anti-windup problem: Its definition and solution", *Proceedings of the 4th ECC*, Brussels, Belgium, July 1997.

[8] A. R. Teel and N. Kapoor, "Uniting local and global controllers", *Proceedings of the 4th ECC*, Brussels, Belgium, July 1997.

[9] A. R. Teel, "Anti-Windup for Exponentially Unstable Linear Systems", *International Journal of Robust and Nonlinear Control*, vol.9, pp. 701-716, 1999.